Inorg. Chem. **2004**, *43*, 7800–7806

A Family of Dioxo–Molybdenum(VI) Complexes of N_2X Heteroscorpionate Ligands of Relevance to Molybdoenzymes

Brian S. Hammes,[†] Bal S. Chohan,[‡] Justin T. Hoffman, Simon Einwächter, and Carl J. Carrano*

Department of Chemistry and Biochemistry, San Diego State University, San Diego, California 92182-1030

Received July 2, 2004

Four new Mo(VI)–dioxo complexes of a family of N_2X heteroscorpionate ligands are reported which, together with data already available for $(Tp^R)^-$, provide a unique example of a comprehensive set of isostructural, isoelectronic complexes differing only in one biologically relevant donor atom. A study of these complexes allows for a direct comparison of structural, spectroscopic, and oxygen atom transfer reactivity properties of the Mo(VI)–dioxo center (of relevance to various families of molybdoenzymes) as a function of donor atom identity.

Introduction

The majority of the mononuclear molybdenum containing enzymes have the general function of catalyzing a net oxygen atom transfer (OAT) to or from a physiological donor/acceptor with the metal cycling between the +6 and +4 oxidation states. They can be conveniently divided into three major groups on the basis of the structure about the metal center, all of which include one or more pterin cofactors.[1] Among the three families, the DMSO reductase family is the most diverse where, in addition to the pterin based ligands, the metal center is often coordinated by endogenous ligation from a serine alkoxide oxygen, a cysteinyl thiolate sulfur, or a carboxylate oxygen from aspartate.[2]

Pyrazolylborate complexes of molybdenum represent a uniquely successful and extensive model system for the pterin dependent molybdoenzymes.[3−10] While in general one would suppose that a 3-fold symmetric, all nitrogen donor ligand would be a poor substitute for the dithiolene and other sulfur donor atoms of these enzymes, they nevertheless provide biomimetic attributes unmatched by other systems. Indeed, hydrido tris(3,5-dimethylpyrazolyl)borate (Tp*) complexes can mimic both the forward and reverse oxygen atom transfer reactions interconverting the Mo(VI) and Mo(IV) states as well as the coupled electron−proton transfer and atom transfer reactions producing the enzymatically important Mo(V) state. In addition, access to stable, mononuclear Mo (VI, V, and IV) complexes has made these systems extraordinarily useful in understanding the electronic structure and redox interplay of the resting and intermediate states of these enzymes.[3−10] Nevertheless, the inherent limitations of these ligands (threefold symmetric with all nitrogen donors) limit their continued utility.

Many of these limitations have been eliminated by our introduction of a family of tripodal N_2X ligands that contain more biologically relevant donor atoms but remain isostructural and isoelectronic with Tp.[11−14] With these ligands, it is

* To whom correspondence should be addressed. E-mail: carrano@sciences.sdsu.edu.

[†] Current address: Department of Chemistry, St. Joseph's University, Philadelphia, PA 19131.

[‡] Current address: Department of Chemistry, Susquehanna University, Selinsgrove, PA 17870.

(1) Hille, R. *Chem. Rev.* **1996**, *96*, 2757−2816.
(2) Stolz, J. F.; Basu, P. *ChemBioChem* **2002**, *3*, 198−206.
(3) Xiao, Z.; Young, C. G.; Enemark, J. H.; Wedd, A. G. *J. Am. Chem. Soc.* **1992**, *114*, 9194−9195.
(4) Laughlin, L. J.; Young, C. Y. *Inorg. Chem.* **1996**, *35*, 1050−1058.
(5) Smith, P. D.; Millar, A. J.; Young, C. G.; Ghosh, A.; Basu, P. *J. Am. Chem. Soc.* **2000**, *122*, 9298−9299.
(6) Nemykin, V. N.; Davie, S. R.; Mondal, S.; Rubie, N.; Somogyi, A.; Kirk, M. L.; Basu, P. *J. Am. Chem. Soc.* **2002**, *124*, 756−757.
(7) Inscore, F. E.; McNaughton, R.; Westcott, B. L.; Helton, M. E.; Jones, R.; Dhawan, I. K.; Enemark, J. H.; Kirk, M. L. *Inorg. Chem.* **1999**, *38*, 1401−1410.
(8) Cleland, W. E.; Barnhart, K. M.; Yamanouchi, K.; Collison, D.; Mabbs, F. E.; Ortega, R. B.; Enemark, J. H. *Inorg. Chem.* **1987**, *26*, 1017−1025.
(9) Roberts, S. A.; Young, C. G.; Kipke, C. A.; Cleland, W. E.; Yamanouchi, K.; Carducci, M. D.; Enemark, J. H. *Inorg. Chem.* **1990**, *29*, 3650. (b) Roberts, S.; Young, C.; Cleland, W.; Ortega, R.; Enemark, J. *Inorg. Chem.* **1990**, *27*, 3044−3051.
(10) Dhawan, I. K.; Pacheco, A.; Enemark, J. H. *J. Am. Chem. Soc.* **1994**, *116*, 7911.
(11) Hammes, B. S.; Carrano, C. J. *Inorg. Chem.* **1999**, *38*, 666.
(12) Hammes, B. S.; Carrano, C. J. *J. Chem. Soc., Dalton Trans.* **2000**, 3304−3309.
(13) Smith, J. N.; Shirin, Z.; Carrano, C. J. *J. Am. Chem. Soc.* **2003**, *125*, 868−869.

10.1021/ic049130p CCC: $27.50
Published on Web 10/23/2004

Scheme 1. Ligands Used in This Study

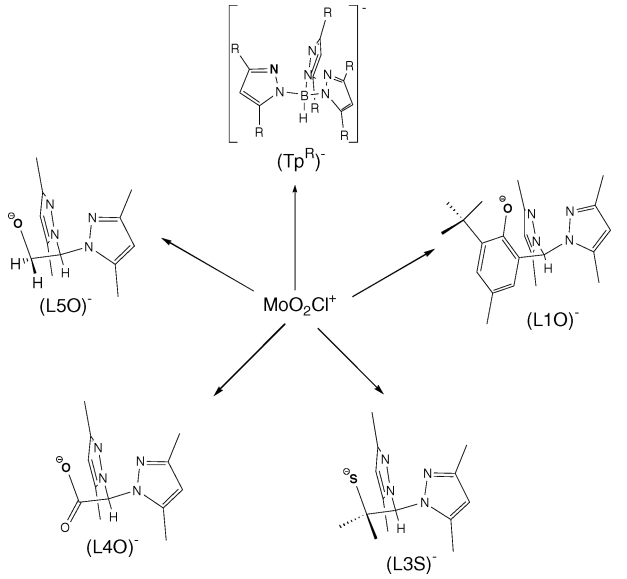

possible to investigate how donor atom identity affects the properties of the metal center in a series of structurally analogous complexes. Complexes of the type [$LMoO_2Cl$] where L = N_2X ligand can exist in two isomeric forms, the *cis* isomer being defined here as the one having a plane of symmetry (i.e., both oxo groups *cis* to the heteroatom). Due to the "*trans*" effect of the oxo atoms, these isomers are expected to differ in a number of important areas including redox potential and OAT reactivity. Thus, a further advantage of our unsymmetrical N_2X ligands is that they provide the potential to explore the effects of geometry on such properties.[15−17]

In this report, we describe the isolation and crystallographic characterization of dioxo Mo(VI) complexes of the entire family of N_2X heteroscorpionate ligands (Scheme 1). Further, we show that the stability of the *cis* or *trans* isomers is dependent on both the nature of the heteroatom donor, X, in the N_2X ligand as well as on the oxidation state of the Mo. These complexes allow a direct comparison of structural, spectroscopic, and reactivity properties of the metal center as a function of donor atom. Given the ubiquity of the parent Tp ligand in bioinorganic and catalytic studies, this approach should have widespread applicability.[18]

Experimental Section

All syntheses were carried out under an inert atmosphere and the reagents and solvents purchased from commercial sources and used as received unless otherwise noted. Subsequent workup was carried out in air. Toluene and THF were distilled under argon over Na/benzophenone. Silica gel 60−200 mesh used in adsorption chromatography and the filtering agent Celite were obtained from the Aldrich Chemical Co. The purity of isolated compounds as well as the progress of the reactions was monitored by thin-layer chromatography. The ligands (3-*tert*-butyl-2-hydroxy-5-methylphenyl)bis(3,5-dimethylpyrazolyl)methane (L1OH) and (2-dimethylethanethiol)bis(3,5-dimethylpyrazolyl)methane (L3SH) and the lithium salt of carboxybis(3,5-dimethylpyrazolyl)methane (L4OLi) were prepared using previously reported procedures.[12,14]

L5OH (1). To a cooled solution (−78 °C) of 22.2 g (0.107 mol) of bis-3,5-dimethylpyrazolylmethane[14] in 200 mL of dry THF was added 40 mL of 2.5 M *n*-butyllithium in hexane. After stirring for 30 min, 6.0 g of paraformaldehyde was added and the solution allowed to come to room temperature. After standing for 48 h, the solution was quenched with 50 mL of 0.1 M HCl, and the THF and water were removed under vacuum. The dry solid was taken up in hot ether and allowed to cool slowly to −28 °C whereupon ca. 5−6 g of the white microcrystalline product precipitated. FTIR (KBr, cm^{-1}): ν_{OH} = 3198 (vs). ^{1}H NMR ($CDCl_3$): δ 6.28 (t, 1 H, J = 6 Hz, −C*H*−), 5.82 (s, 2 H, Pz*H*), 4.39 (d, 2 H, J = 6 Hz, −CH_2−), 2.21 (s, 6 H, Pz−CH_3), 1.94 (s, 6 H, Pz−CH_3). ^{13}C NMR ($CDCl_3$): δ 148.23, 140.34, 106.95, 72.62, 63.29, 13.50, 10.50.

[(L1O)MoO_2Cl] (2). A solution of L1OH (0.49 g, 1.3 mmol) in 15 mL of anhydrous DMF was treated with solid KH (0.054 g, 1.3 mmol). After gas evolution ceased, the K(L1O) solution was added dropwise to a solution of MoO_2Cl_2 in 10 mL of DMF. The resulting mixture was stirred for 1.5 h and filtered to remove a small amount of insoluble material. The filtrate was dried under reduced pressure to give 0.48 g (68%) of [(L1O)MoO_2Cl] (**2**) as a yellow solid. [(L1O)MoO_2Cl] was crystallized by layering a concentrated CH_2Cl_2 solution with hexane. Over a 3 day period, [(L1O)MoO_2Cl] crystallized as yellow needles, which were isolated and dried under reduced pressure. Anal. Calcd (Found) for [(L1O)MoO_2Cl]·CH_2Cl_2, $C_{23}H_{31}N_4O_3Cl_3Mo$: C, 44.99 (45.31); H, 5.10 (4.88); N, 9.12 (9.02). FTIR (KBr, cm^{-1}): ν_{MoO} = 922, 900 (vs). λ_{max} (CH_2Cl_2, ϵ, M^{-1} cm^{-1}): 300 (sh), 344 (3300). ^{1}H NMR ($CDCl_3$): δ 7.16 (d, 2 H, J = 2 Hz, Ar*H*), 6.93 (s, 1 H, −C*H*−), 6.82 (d, 2 H, J = 2 Hz, Ar*H*), 6.02 (s, 2 H, Pz*H*), 2.69 (s, 6 H, Pz−CH_3), 2.48 (s, 6 H, Pz−CH_3), 2.28 (s, 3 H, Ar−CH_3), 1.32 (s, 9 H, −C(CH_3)$_3$). ^{13}C NMR ($CDCl_3$): δ 154.03, 142.46, 140.91, 139.89, 130.28, 129.18, 126.92, 121.75, 108.57, 69.81, 35.26, 30.33, 20.78, 15.01, 11.70.

[(L3S)MoO_2Cl] (3). A solution of L3SH (0.21 g, 0.75 mmol) in 10 mL of anhydrous DMF was treated with solid KH (0.030 g, 0.75 mmol). After gas evolution ceased, the K(L3S) solution was added dropwise to a solution of MoO_2Cl_2 in 10 mL of DMF. The resulting mixture was warmed to 70 °C and stirred for 4 h. Once complete, the reaction mixture was filtered to remove a small amount of insoluble material and dried under reduced pressure to give 0.28 g (84%) of [(L3S)MoO_2Cl] as a orange solid. [(L3S)MoO_2Cl] was crystallized by layering a concentrated CH_2Cl_2 solution with hexane. Anal. Calcd (Found) for [(L3S)MoO_2Cl], $C_{14}H_{21}ClN_4O_2SMo$: C, 38.14 (38.19); H, 4.81 (4.83); N, 12.71 (12.47). FTIR (KBr, cm^{-1}): ν_{MoO} = 928, 896 (vs). λ_{max} (CH_2Cl_2, ϵ, M^{-1} cm^{-1}): 380 (sh), 460 (150). ^{1}H NMR (DMSO-d_6): δ 6.50 (s, 1 H, −C*H*−), 6.29 (s, 2 H, Pz*H*), 2.54 (s, 6 H, Pz−CH_3), 2.51 (s, 6 H, Pz−CH_3), 1.22 (s, 6 H, −C(CH_3)$_2$−). ^{13}C NMR (DMSO-d_6): δ 152.22, 143.07, 107.83, 72.76, 52.20, 29.71, 14.65, 10.88.

[(L4O)MoO_2Cl] (4). A solution of Li(L4O) (1.0 g, 4.0 mmol) in 10 mL of anhydrous DMF was added dropwise to a solution of MoO_2Cl_2 (0.76 g g, 3.8 mmol) in 7.5 mL of DMF. The resulting mixture was stirred overnight. Once complete, the reaction mixture was filtered to remove 0.46 g of a white precipitate. Removal of the DMF from the mother liquor under reduced pressure yielded an additional 0.47 g of product that was washed with acetonitrile

(14) Hammes, B. S.; Kieber-Emmons, M. T.; Latizia, J. A.; Shirin, Z.; Carrano, C. J.; Rheingold, A. L. *Inorg. Chim. Acta* **2003**, 346, 227.
(15) Davie, S. R.; Rubie, N.; Hammes, B. S.; Carrano, C. J.; Kirk, M. L.; Basu, P. *Inorg. Chem.* **2001**, *40*, 2632−2633.
(16) Kail, B.; V. N. Nemykin, V. N.; Davie, S. R.; Carrano, C. J.; Hammes, B. S.; Basu, P. *Inorg. Chem.* **2002**, *41*, 1281−1291.
(17) Hoffman, J. T.; Einwaechter, S.; Chohan, B. S.; Basu, P.; Carrano, C. J. *Inorg. Chem.*, in press.
(18) Trofimenko, S. *Scorpionates: The Coordination Chemistry of Polypyrazolylborate Ligands*; Imperial College Press: London, U.K., 1999.

Table 1. Summary of Crystallographic Data and Parameters for $[(L1O)Mo)_2Cl]\cdot CH_2Cl_2$ (**2**·CH_2Cl_2), $[(L3S)MoO_2Cl]$ (**3**), $[(L4O)MoO_2Cl]$ (**4**), and $[(L5O)MoO_2Cl]$ (**5**)

	2	**3**	**4**	**5**
molecular formula	$C_{22}H_{29}N_4O_3ClMo$	$C_{14}H_{21}N_4SO_2ClMo$	$C_{12}H_{19}N_4O_4ClMo$	$C_{12}H_{17}N_4O_3ClMo$
fw	611.80	440.84	414.70	396.68
temp (K)	293(2)	293(2)	100(2)	203(2)
cryst syst	rhombohedral	orthorhombic	triclinic	monoclinic
space group	*R*3*m*	$P2_12_12_1$	$P\bar{1}$	$P2_1/c$
cell constants				
a (Å)	27.700(3)	8.658(2)	8.028(1)	7.873(1)
b (Å)	27.700(3)	13.397(3)	9.754(1)	11.539(2)
c (Å)	9.143(2)	15.147(4)	10.445(1)	16.266(3)
α (deg)	90	90	76.584(2)	90
β (deg)	90	90	67.670(2)	96.564(14)
γ (deg)	120	90	87.748(2)	90
Z	18	4	2	4
V (Å^3)	6076(2)	1757.0(7)	734.82(16)	1468.1(5)
abs coeff, μ_{calc} (mm^{-1})	0.814	1.031	1.099	1.099
δ_{calc} (g/cm^3)	1.505	1.670	1.874	1.867
F(000)	2808	900	420	832
cryst dimens (mm^3)	0.9 × 0.4 × 0.2	0.8 × 0.6 × 0.2	0.19 × 0.16 × 0.06	0.2 × 0.4 × 0.4
radiation	Mo Kα (λ = 0.71073 Å)	Mo Kα (λ = 0.71073 Å)	Mo Kα (λ = 0.71073 Å)	Mo Kα (λ = 0.71073 Å)
h, *k*, *l* ranges colled	−29 → 0 −9 → 29 −7 → 9	0 → 9 −14 → 0 0 → 16	−8 → 8 −10 → 10 −11 → 11	0 → 8 0 → 10 −17 → 17
θ range (deg)	2.38−22.48	2.03−22.50	2.15−23.50	2.17−22.50
no. reflns collected	2766	1336	4477	1929
no. unique reflns	1778	1336	2119	1787
no. params	178	209	199	199
data/param ratio	9.99	6.39	10.65	8.98
refinement method	full-matrix least-squares of F^2	full-matrix least-squares of F^2	full-matrix least-squares of F^2	full-matrix least-squares of F^2
$R(F)^a$	0.0503	0.0542	0.0892	0.0396
$R_w(F^2)^b$	0.1266	0.1587	0.2211	0.1009
GOFw^c	0.988	1.101	0.997	1.127
largest diff peak and hole (e/Å^3)	0.774 and −0.601	0.826 and −0.503	4.454 and −2.481	0.562 and −0.601

[a] $R = [|\Delta F|/|F_o|]$. [b] $R_w = [w(\Delta F)^2/wF_o^2]$. [c] Goodness of fit on F^2.

and dried under reduced pressure to give a total yield of 0.93 g (57%) of $[(L4O)MoO_2Cl]$ as a white solid. $[(L4O)MoO_2Cl]$ was crystallized by layering a concentrated CH_2Cl_2 solution with isopropyl ether. Anal. Calcd (Found) for $[(L4O)MoO_2Cl]$, $C_{12}H_{15}ClN_4O_4Mo$: C, 35.10 (34.88); H, 3.68 (3.60); N, 13.64 (13.45). FTIR (KBr, cm^{-1}): ν_{MoO} = 941, 910 (vs). ^{1}H NMR (DMSO-d_6): δ 7.11 (s, 1 H, −C*H*−), 5.86 (s, 2 H, Pz*H*), 2.17 (s, 6 H, Pz−CH_3), 2.07 (s, 6 H, Pz−CH_3). ^{13}C NMR (DMSO-d_6): δ 165.93, 146.82, 140.54 106.42, 71.43, 13.22, 10.79.

[(L5O)MoO$_2$Cl] (5). A solution of **1** (0.31 g, 1.3 mmol) in 15 mL of anhydrous DMF was treated with solid KH (0.054 g, 1.3 mmol). After gas evolution ceased, the K(L5O) solution was added dropwise to a DMF solution of MoO_2Cl_2 (0.27 g, 1.3 mmol). The resulting mixture was warmed to 70 °C and stirred for 4 h. Once complete, the reaction mixture was filtered to remove a small amount of insoluble material and dried under reduced pressure. $[(L5O)Mo(O)_2Cl]$ (**5**) was crystallized by layering a concentrated CH_2Cl_2 solution with hexane to give 0.15 g (28%) of **5** as light yellow blocks. Anal. Calcd (Found) for $[(L5O)MoO_2Cl]$, $C_{12}H_{17}ClN_4O_3Mo$: C, 36.33 (36.37); H, 4.33 (4.22); N, 14.12 (14.02). FTIR (KBr, cm^{-1}): ν_{MoO} = 937, 908 (vs). ^{1}H NMR (CD_3CN): δ 6.69 (t, 1 H, J = 2 Hz, −C*H*−), 6.11 (s, 2 H, Pz*H*), 4.65 (d, 2 H, J = 2 Hz, −CH_2−), 2.51 (s, 6 H, Pz−CH_3), 2.44 (s, 6 H, Pz−CH_3). ^{13}C NMR (CD_3CN): δ 153.35, 141.74, 108.25, 73.28, 66.16, 14.48, 11.07.

Physical Methods. Elemental analyses were performed on all compounds by Quantitative Technologies, Inc., Whitehouse, NJ. All samples were dried in vacuo prior to analysis. The presence of solvates was corroborated by FTIR, ^{1}H NMR, or X-ray crystallography. ^{1}H and ^{13}C NMR spectra were collected on a Varian UNITY INOVA 400 or 500 MHz NMR spectrometers. Chemical shifts are reported in ppm relative to an internal standard of TMS. The ^{13}C quaternary carbon peaks that are not observed are a result of either poor solubility and/or overlapping signals. IR spectra were recorded as KBr disks on a Perkin-Elmer Spectrum One or a ThermoNicolet Nexus 670 FT-IR spectrometer and are reported in wavenumbers. Cyclic voltammetric experiments were conducted using a BAS CV 50W (Bioanalytical Systems Inc., West Lafayette, IN) voltammetric analyzer. All experiments were done under argon at ambient temperature in solutions with 0.1 M tetrabutylammonium hexafluorophosphate as the supporting electrolyte. Cyclic voltammograms (CV) were obtained using a three-electrode system consisting of glassy-carbon working, platinum wire auxiliary, and SCE reference electrodes. The ferrocenium/ferrocene couple was used to monitor the reference electrode and was observed at 0.768 V with ΔE_p = 0.120 V and $i_{pc}/i_{pa} \cong 1.0$ in CH_2Cl_2 under these conditions. IR compensation was applied before each CV was recorded. Potentials are reported versus the saturated calomel couple. Electronic spectra were recorded using a Cary 50 UV−vis spectrophotometer.

Reactivity Studies. $[LMoO_2Cl]$ complexes undergo oxygen atom transfer reactions with Ph_3P in pyridine to produce Ph_3PO and [LMoOCl(py)]. This reaction was investigated under pseudo-first-order reaction conditions using a 500-fold excess of Ph_3P at 30(1) °C. All reactions were run in triplicate at a concentration of 2.5 mM $[LMoO_2Cl]$ in anhydrous pyridine. Solutions were equilibrated at 30 °C prior to initiation of the reaction by addition of the phosphine via gastight syringe. The reaction was monitored at 700 nm using a Cary 50 UV−vis spectrometer with a jacketed cell attached to a constant temperature circulating bath. Rate constants

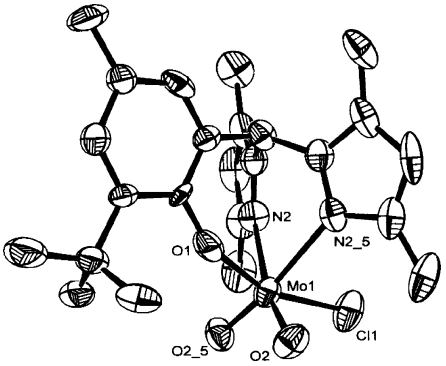

Figure 1. ORTEP diagram with 50% thermal ellipsoids of [(L1O)MoO_2Cl] (**2**) showing selected atomic labeling.

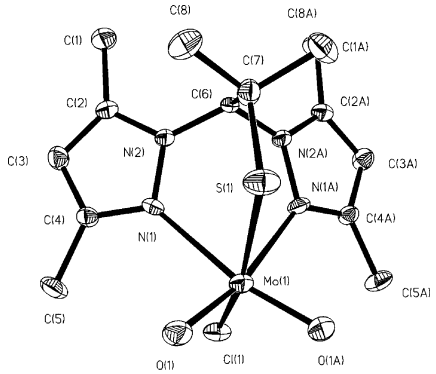

Figure 2. ORTEP diagram with 50% thermal ellipsoids of [(L3S)MoO_2Cl] (**3**) showing complete atomic labeling.

were calculated using the scanning kinetics program included with the instrument software. Isosbestic points were generally not observed in the reactions due to the coincident formation of a species that absorbs in the 425 nm region (approximately where it appears the isosbestic points would occur). This species, whose formation is not unprecedented and has been reported previously, is due to a side reaction with the Ph_3P.[9b]

Computational Details. All of the density functional calculations were performed using Becke's three-parameter hybrid exchange functional and the Lee−Yang−Parr nonlocal correlation functional (B3LYP) within the borders of unrestricted and restricted open Hartree-Hock formalism, without symmetry restrictions. For both optimized geometries and single point calculations, a B3LYP exchange-correlation functional with a 6-31G** basis set for all non-ECP atoms and a LACVP** effective core potential on heavy atoms were employed. All single point and geometry optimized DFT calculations were performed using the program Jaguar (Schroedinger) running under a Linux operating system.

Crystallographic Structure Determination. Crystal, data collection, and refinement parameters for **2**−**5** are given in Table 1. Crystals of all complexes were sealed in thin-walled quartz capillaries, and data collection was initiated at 293 K except for **4** which was mounted on a fiber and cooled to 213 K. Data were collected on a Siemens P4 diffractometer with a sealed-tube Mo X-ray source and controlled via PC computer running Siemens XSCANS 2.1 again except for compound **4** which was collected on a Bruker SMART APEX at UCSD. The systematic absences in the diffraction data are consistent with the space groups *R*3*m* for [(L1O)MoO_2Cl] (**2**), $P2_12_12_1$ for [(L3S)MoO_2Cl]·CH_2Cl_2 (**3**·CH_2Cl_2), $P\bar{1}$ for **4**, and $P2_1/c$ for **5**. The structures were solved using direct methods or via the Patterson function, completed by subsequent difference Fourier syntheses, and refined by full-matrix least-squares procedures on F^2. The asymmetric unit of **3** contained a well ordered molecule of CH_2Cl_2. All non-hydrogen atoms were refined with anisotropic displacement coefficients, while hydrogen atoms were treated as idealized contributions using a riding model except where noted. All software and sources of the scattering factors are contained in the SHELXTL (6.0) program library (G. Sheldrick, Bruker AXS, Madison, WI). The single-crystal X-ray crystallographic data for each of the complexes are found in Figures 1−4 and Table 1. Selected bond lengths are found in Table 2 while more complete bond length and angle data are given in Tables S1−S4 of Supporting Information.

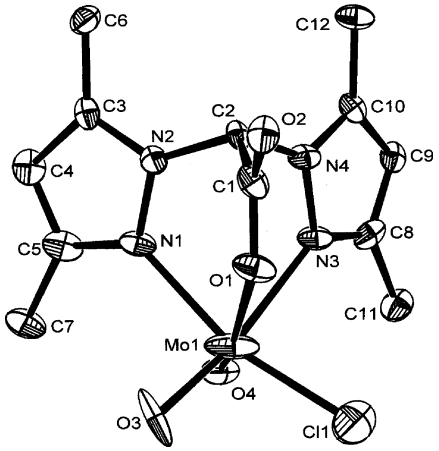

Figure 3. ORTEP diagram with 50% thermal ellipsoids of [(L4O)MoOCl_2] (**4**) showing complete atomic labeling.

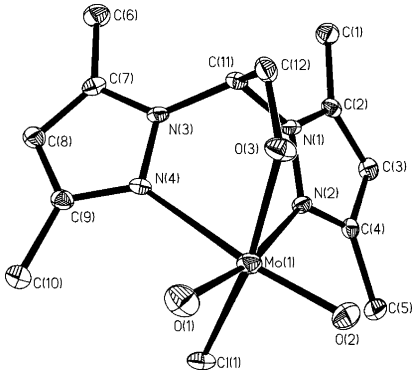

Figure 4. ORTEP diagram with 50% thermal ellipsoids of [(L5O)MoOCl_2] (**5**) showing complete atomic labeling.

Table 2. Bond Distances from the DFT Optimized Geometries and X-ray Crystallography

isomer	Mo═O	Mo═O	Mo−N	Mo−N	Mo−Cl	Mo−X
cis (L1O)	1.714	1.714	2.435	2.436	2.415	1.949
expt	1.710(6)	1.710(6)	2.373(8)	2.373(8)	2.373(3)	1.898(9)
trans (L1O)	1.711	1.722	2.298	2.503	2.378	2.012
cis (L3S)	1.712	1.712	2.437	2.434	2.417	2.475
expt	1.694(6)	1.694(6)	2.346(7)	2.346(7)	2.384(4)	2.421(4)
trans (L3S)	1.708	1.729	2.301	2.509	2.361	2.531
cis (L5O)	1.713	1.713	2.459	2.459	2.412	1.957
expt	1.697(4)	1.696(4)	2.354(5)	2.374(5)	2.395(2)	1.911(4)
trans (L5O)	1.710	1.724	2.317	2.558	2.369	1.990
cis (L4O)	1.708	1.708	2.430	2.432	2.383	2.035
expt	1.754(8)	1.769(7)	2.212(9)	2.323(9)	2.233(4)	2.130(7)
trans (L4O)	1.706	1.718	2.276	2.475	2.346	2.100

Results

Synthesis. All the ligands of the family have been prepared by one of two routes, i.e., reaction of a dipyrazole ketone

with an aldehyde in the presence of $CoCl_2$ as a catalyst (L1O and L3S series) or by lithiation of a dipyrazolylmethane followed by quenching with the appropriate electrophile (L4O and L5O series). Six-coordinate dioxo−Mo(VI) complexes, [(L1O)MoO_2Cl] **1**, [(L3S)MoO_2Cl] **2**, [(L4O)MoO_2Cl] **3**, or [(L5O)MoO_2Cl] **4**, were readily prepared by direct reaction of deprotonated ligand (KH) with a stoichiometric quantity of MoO_2Cl_2 in anhydrous DMF. Disappointing and somewhat surprising was the fact that we were unable to effect substitution chemistry at the chloride in any of these complexes using methodology that was successful in the related Tp^R series. Thus, refluxing **1** in a variety of solvents with either K^+X^- or HX plus triethylamine led to no observable product formation. Treatment of **1** with silver salts to remove the chloride followed by addition of K^+X^- or HX plus triethylamine were also unavailing. One methodology that offers some hope is based on the observation that reaction of $MoO_2(acac)_2$ with L1OH in methanol cleanly produces [(L1O)MoO_2OCH_3] whose methoxide ion might be substitutable by proton transfer with an HX more acidic than methanol. Details will be reported in a subsequent publication.

Solid State Structures. The structures of complexes **2**−**5** are unexceptional, being very similar to each other and to analogous dioxo Mo(VI) species. Thus, the molybdenum oxygen multiple bonds are all near 1.7 Å, although the Mo−N values from the pyrazoles are somewhat longer than a "normal" Mo−N bond and average 2.36 Å (expected ca. 2.2 Å) due to the *trans* influence of the oxo groups. The only substantial difference between the structures is the varying bond length of the M−X heteroatom bond that ranges from 1.8 Å (for the phenolate oxygen of **2**) to 2.46 Å (for the thiolate sulfur of **3**). The stereochemistry of each of the complexes is *cis* except for compound **4** where an analysis of the bond lengths suggests a compositional disorder between the oxo group and the chlorides consistent with a mixture of *cis* and *trans* isomers being present but with the *trans* predominating. This leads to longer than expected molybdenum oxygen multiple bonds (1.76 Å) and shorter than expected Mo−Cl bonds (2.23 Å). This phenomenon, which had previously been dubbed "bond stretch isomerization", is now known to be a common effect of solid solutions of mixed isomers.[19−21]

Isomerization. One of the useful features of our heteroscorpionate ligands is that stereoisomers can be present and isolated (the *cis* isomer being defined here as the isomer with the oxo groups cis to the heteroatom in the N_2X ligand, the *trans* isomer has one oxo group trans to the heteroatom donor). The two isomers are easily distinguished by NMR since the *cis* isomer possesses a plane of symmetry while the *trans* isomer is asymmetric. In all cases, ^{1}H NMR spectra demonstrate that in d_6-DMSO solution the *cis* isomer is preferred, which is consistent with the solid state results for all complexes except **4** (vide infra).

Table 3. Calculated (DFT) Difference in Energy, *cis* over *trans* for $LMoO_2Cl$ Complexes

ligand	ΔE (kcal/mol)
L3S (thiolate)	8.04
L5O(alkoxide)	4.60
L1O(phenolate)	4.10
L4O (carboxylate)	2.58

Because the X-ray crystal structures are not available for all the *cis*/*trans* pairs of the [$LMoO_2Cl$] series, an understanding of the possible influence of the *trans* effect of the oxo group upon the geometry and stability of these complexes is possible only through a modern DFT computational approach. In order to compare the predicted stabilities of the *cis* versus *trans* isomers, both isomers of each ligand were first geometry optimized starting from the crystallographic data where available. Relative energies of the two isomers were then calculated at the optimized geometry. The most important bond distances in the optimized geometries of all of the eight possible structures (i.e., *cis* and *trans* [(L1O)MoO_2Cl], [(L3S)MoO_2Cl], [(L4O)MoO_2Cl], and [(L5O)MoO_2Cl]) are presented in Table 2. When possible, a comparison of the X-ray determined structure and the optimized geometry was made and found to be in good agreement (although the basis set used here typically gave Mo−X bonds consistently ca. 0.05 Å longer than the crystallographically derived values). Single point energy calculations at the optimized geometries support the notion that in the dioxo Mo(VI) species the thermodynamically more stable isomer should be the *cis* in all cases but that the energy difference between *cis* and *trans* is smallest for the L4O ligand found in complex **4** (Table 3). This is in contrast to the case for monooxo Mo(V) where the *trans* isomer (defined as the isomer with the lone oxo group *trans* to the heteroatom donor) is predicted and experimentally verified to be the more stable isomer for the phenoxy ligand, L1O, and a derivative of the alkoxy ligand L5O.[15,16] Thus, there are both oxidation state and donor atom dependent differences in isomeric stability. While the X-ray structure of **4** was compositionally disordered, the nature of the disorder suggested that the *trans* isomer was predominant. Thus, we were puzzled when the NMR spectrum of **4** in d_6-DMSO revealed only the presence of the symmetrical *cis* isomer. Reasoning that since the energy difference between the *cis* and *trans* isomers (as revealed by the gas phase DFT calculations) was small for ligand $L4O^-$ that the isomer preference could be tipped by effects such as solvation, we recorded a spectrum of **4** in CD_2Cl_2 that showed the almost exclusive presence of the asymmetric *trans* isomer (Figure 5). Recording spectra in several other solvents revealed the presence of a mixture.

Electrochemistry. Not unexpectedly, the redox potential of these complexes is strongly modulated by the nature of the heteroatom donor as revealed in Table 4. Thus, the phenolate and alkoxy oxygens, which are capable of π-bonding interactions with the Mo and lead to short Mo−O bonds due to significant multiple bond character, stabilize the

(19) Yoon, K.; Parkin, G.; Rheingold, A. L. *J. Am. Chem. Soc.* **1991**, *113*, 1437.
(20) Desrochers, P. J.; Nebesny, K. W.; LaBarre, M. J.; Lincoln, S. E.; Loehr, T. M.; Enemark, J. H. *J. Am Chem. Soc.* **1991**, *113*, 9193.
(21) Parkin, G. *Chem. Rev.* **1993**, *93*, 887.

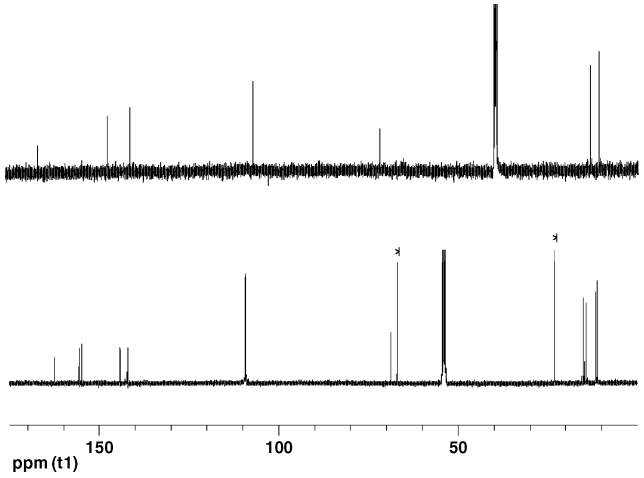

Figure 5. ^{13}C NMR spectra of **4** in d_6-DMSO (upper) and CD_2Cl_2 (lower). The peaks marked with the asterisk are from residual isopropyl ether.

Table 4. Redox Potentials[a] and OAT Reactivity of [$LMoO_2Cl$] Complexes

ligand	$E°$ vs SCE (V)	i_{pa}/i_{pc}	relative rate of OAT
L1O	−1.16	irr	2.14
L5O	−1.15	0.10	1.00
L3S	−0.83	irr	278
L4O	−0.65	0.90	15.7
Tp*	−0.62	0.60	1360[b]

[a] 0.1 M $TBAPF_6$ in CH_2Cl_2, 200 mV/s. [b] Estimate only as rate is too fast for quantitative measurement.

Mo(VI) state while the carboxylate oxygen of **4** results in a complex that is almost 0.5 V easier to reduce. The nitrogen and sulfur donors of Tp* and L3S give redox potentials within 200 mV of the oxygen donor complex **4**. Thus, on going from phenoxide/alkoxide oxygens through thiolate sulfur to carboxylate oxygen or aromatic nitrogen it becomes progressively easier to reduce Mo(VI) lending support to the notion that one of the roles of the exogenous protein donor ligands in the molybdoenzymes is to help poise the redox potential at an appropriate value.

OAT Reactions. In order to compare the oxygen atom transfer capabilities of these complexes, we examined their reactivity in pyridine at 30 °C with triphenylphosphine as an acceptor. The results are depicted in Table 4. The rates of OAT transfer vary by over 3 orders of magnitude as a function of donor atom identity. Thus, the alkoxy and phenoxy complexes are poor OAT transfer reagents with relative rates near 1 while the complex with Tp* reacts at least 1300 times faster. The complexes with the thiolate ligand L3S and the carboxylate ligand L4O have intermediate values.

Since the molybdenum center in all the molybdopterin enzymes cycle is between the +6 and +4 oxidation states during oxygen atom transfer, it is reasonable to suppose that there should be a correlation between the rate of OAT and redox potential. Although one cannot in general measure the relevant $2e^-$ Mo(VI)/(IV) redox potential directly, it has been demonstrated that a terminal oxo group so dominates the ligand field in these complexes that it invariably results in an energetically isolated d_{xy} redox orbital.[3,22,23] Therefore,

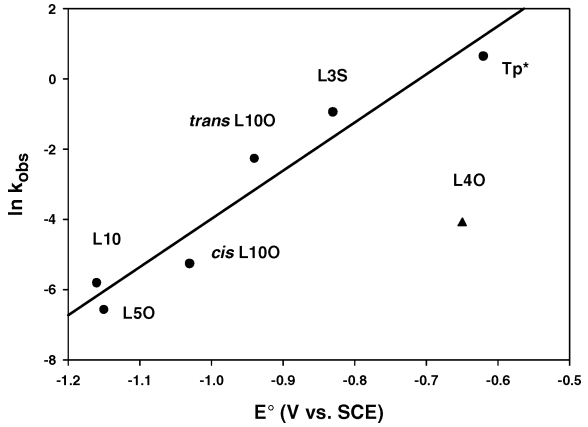

Figure 6. Plot of redox potential (vs SCE) verses natural logarithm of the rate of oxygen atom transfer. Conditions as described in the text.

both the (VI)/(V) or (V)/(IV) reduction potentials of oxo−molybdenum centers follow the same trends which are intimately related to the valence ionization energy of this orbital.[22] Thus, as has previously been noted, the relative efficiency of OAT to triphenylphosphine generally follows the observed redox potentials, and a reasonable linear correlation exists between the Mo(VI)/Mo(V) redox potential and the natural logarithm of the rate of OAT (Figure 6).[23] The clear exception to the linear trend line is compound **4** whose OAT reactivity is anomalously low. At the moment, we cannot account for this observation except to say that **4** is anomalous in many other respects (vide supra).

Conclusions. There is increasing evidence that metal-based isomerizations may play an important role in the mechanism of some molybdoenzymes.[24−26] The data presented here indicates that there are both oxidation state and donor atom dependencies in the relative stabilities of the *cis* and *trans* isomers of oxo−Mo centers. This is important given the "oxo-gate hypothesis" and numerous theoretical studies that indicate that the precise geometric relationship between the pterin sulfurs and/or protein backbone ligands with respect to the Mo oxo groups has important effects on electron transfer gating, redox potential, and OAT reactivity.[27]

Acknowledgment. This work was supported in part by Grants CHE-0313865 and CHE-0202535 from the NSF. The NSF-MRI program Grant CHE-0320848 is acknowledged for support of the X-ray diffraction facilities at San Diego State University. Professor Arnie Rheingold, Department of

(22) Izumi, Y.; Glaser, T.; Rose, K.; McMaster, J.; Basu, P.; Enemark, J. H.; Hedman, B.; Hodgson, K. O.; Solomon, E. I. *J. Am. Chem. Soc.* **1999**, *121*, 10035.
(23) Enemark, J. H.; Cooney, J. J. A.; Wang, J.; Holm, R. H. *Chem. Rev.* **2004**, *104*, 1175−1200.
(24) George, G. N.; Mertens, J. A.; Campbell, W. H. *J. Am. Chem. Soc.* **1999**, *121*, 9730.
(25) Heffron, K.; Leger, C.; Rothery, R. A.; Weiner, J. H.; Armstrong, F. A. *Biochemistry* **2001**, *40*, 3117.
(26) Peariso, K.; Chohan, B. S.; Carrano, C. J.; Kirk, M. L. *Inorg. Chem.* **2003**, *42*, 6194.
(27) McNaughton, R. L.; Helton, M. E.; Rubie, N. D.; Kirk, M. L. *Inorg. Chem.* **2000**, *39*, 4386−4387.

Chemistry and Biochemistry, University of California San Diego, is gratefully acknowledged for X-ray data collection on **4**. We thank Professors Marty Kirk, University of New Mexico, and Partha Basu, Duquesne University, for valuable discussions.

Supporting Information Available: Tables of selected bond lengths and angles for **2**−**5**. Additional crystallographic data (CIF files) for **2**−**5**. This material is free of charge via the Internet at http://pubs.acs.org.

IC049130P